We are IntechOpen, the world's leading publisher of Open Access books Built by scientists, for scientists

4,800
Open access books available

122,000
International authors and editors

135M
Downloads

Our authors are among the

154
Countries delivered to

TOP 1%
most cited scientists

12.2%
Contributors from top 500 universities

CLARIVATE ANALYTICS BOOK CITATION INDEX INDEXED

WEB OF SCIENCE™

Selection of our books indexed in the Book Citation Index in Web of Science™ Core Collection (BKCI)

Interested in publishing with us?
Contact book.department@intechopen.com

Numbers displayed above are based on latest data collected.
For more information visit www.intechopen.com

22

A SIFT-Based Fingerprint Verification System Using Cellular Neural Networks

Giancarlo Iannizzotto and Francesco La Rosa
University of Messina (VisiLAB)
Italy

1. Introduction

Recently, with the increasing demand of high security, person identification has become more and more important in our everyday life. The purpose of establishing the identity is to ensure that only a legitimate user, and not anyone else, accesses the rendered services. The traditional identification methods are based on "*something that you possess*" and "*something that you know*" such as key, user-ID, password, PIN, etc. Examples of such applications include secure access to buildings, airports, computer systems, cellular phones and ATM machines. Another family of identification methods uses biometric characteristics. Biometric recognition, or simply *biometrics*, refers to the automatic recognition of individuals based on their physiological and/or behavioral characteristics. Biometrics allows us to confirm or establish an individual's identity based on *who she is*, rather than by *what she possesses* (e.g., an ID card) or *what she knows* (e.g., a password). Current biometric systems make use of identifiers such as fingerprints, hand geometry, iris, face and voice to establish an identity. Biometric systems also introduce an aspect of user convenience. For example, they alleviate the need for a user to remember multiple passwords associated with different applications.
Fingerprint characterization is the oldest and the prevalent member of the biometric family and has been extensively used for person identification in a number of commercial, civil and forensic applications.
The question that is being asked about biometric technologies in general and about fingerprints in particular is that whether these technologies can work all the time, everywhere, and in all contexts for reliable person identification and authentication.
One of the design criteria for building such completely automatic and reliable fingerprint identification (and verification) systems is that the underlying sensing, representation, and matching technologies must also be very robust.
In practice, due to variations in impression conditions, ridge configuration, skin conditions (aberrant formations of epidermal ridges of fingerprints, postnatal marks, occupational marks), acquisition devices and non-cooperative attitude of subjects a significant percentage of acquired fingerprint images is of poor quality. In order to ensure that the performance of a feature extraction algorithm will be robust with respect to the quality of input fingerprint images, an enhancement algorithm which can improve the clarity of the ridge structures is useful. Most of the fingerprint image enhancement methods (Gabor, directional or anisotropic filter based) use convolution to obtain the results. Another way to address these

Source: Pattern Recognition Techniques, Technology and Applications, Book edited by: Peng-Yeng Yin,
ISBN 978-953-7619-24-4, pp. 626, November 2008, I-Tech, Vienna, Austria

requirements of robust performance is to adopt robust representation schemes that capture the discriminatory information in fingerprint impressions.
Also, thanks to the increasing power of computers and to the substantial improvement in capture devices, the use of fingerprint for personal identification in portable applications is very significant.
For purpose of commercialization, a fingerprint verification system has to take the following four crucial factors into consideration: *processing speed*, *recognition rate*, *power consumption* and *size*. These approaches described are computationally very expensive tasks.
An alternative to the traditional approaches is provided by the *Cellular Neural Network* (CNN) paradigm, introduced by Prof. L.O. Chua in 1988 (Chua & Yang, 1988a; 1988b). A CNN consists of a network of first order nonlinear circuits, locally interconnected by linear (resistive) connections.
The rapidly growing field of Cellular Neural Networks (CNNs) and analogic cellular computing CNN-UM (Chua & Roska, 1993) has found a number of potential applications (Chua & Yang, 1988b), especially in image and video processing problems (Moreira-Tamayos & Gyvez, 1999; Iannizzotto et al., 2005, Costantini et al., 2004) where real-time signal processing is required. This architecture provides an efficient tool to explore the rich world of dynamical systems and makes possible to introduce new approaches for pattern recognition (Szirànyi & Csicsvàri, 1993; Theodoridis & Koutroumbas, 2006) and object classification (Milanova & Buker, 2000; Bálya, 2003), relevant problems in image processing.
CNNs can process information at very high speeds comparable to today's supercomputers. The regular lattice architecture of CNNs allows massive parallelism that makes it very suitable for performance-demanding applications in image processing.
Fingerprint-based identification (and verification) systems using CNNs are very promising for personal identification and in particular, if incorporated in a VLSI chip, for use in portable applications.
They have the potential to *realize a fingerprint-based identification (or verification) system on one chip* assuming that it is possible to incorporate a capacitive or optical sensor on the same chip.
Various approaches to implement real-time person verification and identification systems on CNNs have been proposed (Su et al., 2006; Gao et al., 2001; Gao & Moschytz, 2001; 2004). However in (Su et al., 2006) the level of accuracy and robustness of the fingerprint verification system was not investigated and in (Gao & Moschytz, 2004) are not used public domain fingerprint databases.
The most popular method for fingerprint representation is based on local landmarks called minutiae. The minutiae-based systems first locate the points, often referred as minutiae points, in fingerprint image where the fingerprint ridges either terminate or bifurcate (see fig. 1) and then match minutiae relative placement in a given finger and the stored template (Jain et al., 1997).
While minutiae-based fingerprint verification systems have shown to be fairly accurate, further improvements are needed for acceptable performance, especially in applications involving very large scale databases.
The aim of this chapter is to re-formulate an algorithm for fingerprint verification using Scale Invariant Feature Transform (SIFT) (Lowe 1999; Lowe, 2004; Park et al., 2008) in such a way to exploit the high degree of parallelism inherent in a single-layer CNN.
SIFT detects and describes local features in images. The SIFT features are local and based on the appearance of the object at particular interest points and are invariant to image scale and rotation. They are also robust to changes in illumination, noise, occlusion and minor changes in viewpoint. In addition, the SIFT features are discriminant and allow for correct

object identification with low probability of mismatch and are easy to match against a (*large*) database of local features (Bicego et al., 2006).

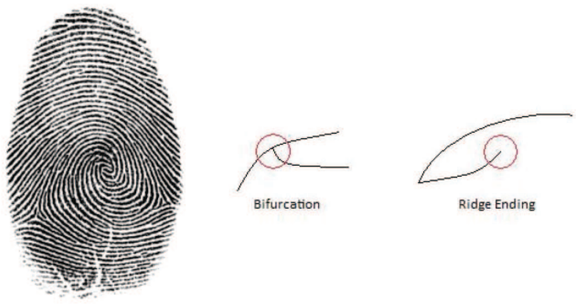

Fig. 1. An example of bifurcation and ridge ending in a fingerprint image

In our implementation we extract characteristic SIFT feature points in scale space and perform a matching based on the texture information around the feature points using the SIFT operator (Chikkerur, 2006).

The input to the system is a gray level fingerprint image where a number of feature points (*keypoints*) are located using a difference-of-Gaussian function in a scale space. A descriptor, representing each feature point and invariant to rotation, scale and change of lighting, is calculated.

In this chapter we describe the technique developed and present a set of experimental results. In the final section we draw our conclusions on the work carried out.

2. Scale invariant feature transform

There are three typical categories of fingerprint verification methods: i) minutiae, ii) correlation, and iii) ridge features. However, considering the types of information used, a method can be broadly categorized as minutiae based or texture based. While the minutiae based fingerprint verification systems have shown high accuracy (Jain et al., 1997; Ratha et al., 1996), they ignore the rich information in ridge patterns which can be useful to improve the matching accuracy. Most of the texture based matchers use the entire fingerprint image or local texture around minutiae points (Chikkerur et al., 2006). Using local texture is more desirable because the global texture will be more sensitive to non-linear and non-repeatable deformation of fingerprint images. When the local texture is collected based on the minutiae points, the texture based fingerprint representation is again limited and its performance depends upon the reliability of extracted minutiae points. It is not obvious how one could capture the rich discriminatory texture information in the fingerprints that is not critically dependent on finding minutiae points or core points.

For the purpose of extending characteristic feature points of fingerprint beyond minutiae points, we adopt Scale Invariant Feature Transform (SIFT) (Lowe, 2004). SIFT extracts repeatable characteristic feature points from an image and generates descriptors representing the texture around the feature points. In (Park, 2008) the authors have demonstrated the utility of SIFT representation for fingerprint-based identification. As the SIFT feature points have already demonstrated their efficacy in generic object recognition problems, in the same way this representation is also stable and reliable for many of the matching problems related to the fingerprint domain. Further, since SIFT feature points are

based on texture analysis of the entire scale space, these feature points are probably robust to the fingerprint quality and deformation variation.
The features are selected to be invariant to image scale and rotation, and to provide robust matching across a substantial range of affine distortion, addition of noise and partial change in lighting.
The features are highly distinctive, in the sense that a single feature can be correctly matched with high probability against a large database of features from many images, providing a basis for object and scene recognition. In the original implementation, the recognition proceeds by matching individual features to a database of features from known objects using a fast nearest-neighbour algorithm, followed by a generalized Hough transform to identify clusters belonging to a single object, and finally performing verification through least-squares solution for consistent pose parameters.
Following are the major stages of computation used to generate the set of image features:

- **Scale-space extrema detection:** to identify potential interest points invariant to scale it's used a difference-of-Gaussian function (see fig.2).
- **Keypoint localization:** at each candidate location, a detailed model is fit to determine location and scale. Keypoints are selected based on measures of their stability.
- **Orientation assignment: o**ne or more orientations are assigned to each keypoint location based on local image gradient directions. All future operations are performed on image data that has been transformed relative to the assigned orientation (providing invariance to these transformations).
- **Keypoint descriptor:** the local image gradients are measured at the selected scale in the region around each keypoint. These are transformed into a representation that allows for significant levels of local shape distortion and change in illumination.

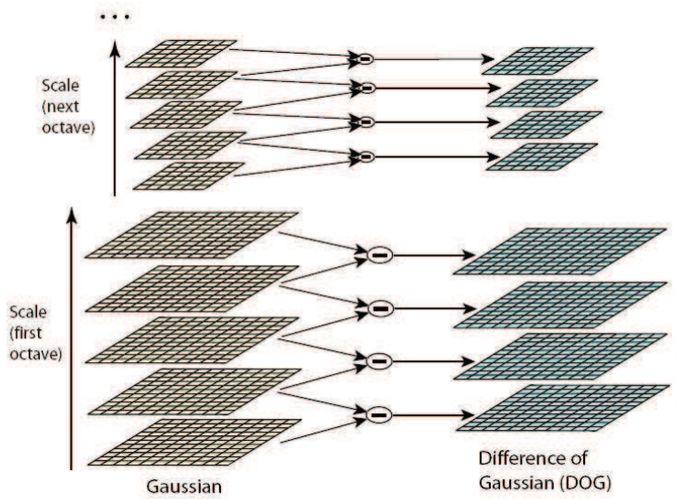

Fig. 2. Scale-space extrema detection

This approach has been named Scale Invariant Feature Transform (**SIFT**), as it transforms image data into scale-invariant coordinates relative to local features.
An important property of this approach is that it generates large numbers of features that densely cover the image over the full range of scales and locations. A typical image of size 500x500 pixels will give rise to about 2000 stable features (although this number depends on both image content and choices for various parameters). The quantity of features is

particularly important for object recognition, where the ability to detect small objects in cluttered backgrounds requires that at least 3 features be correctly matched from each object for reliable identification.
For image matching and recognition, SIFT features are first extracted from a set of reference images and stored in a database. A new image is matched by individually comparing each feature from the new image to this previous database. In seminal work of Lowe (Lowe, 1999) the finding candidate matching features is based on Euclidean distance of their feature vectors. Specifically, a fast nearest-neighbour algorithm is used to perform this computation rapidly against large databases. In our implementation, we have evaluated two different metrics: the Lowe and Szatmári (Szatmári, 2006) metrics.

3. Cellular Neural Network

As stated in the introduction, a CNN consists of an array of non-linear, locally interconnected, first order circuits. As connections are local, each cell is connected only to the cells belonging to its neighbourhood, as it is shown in fig.3.

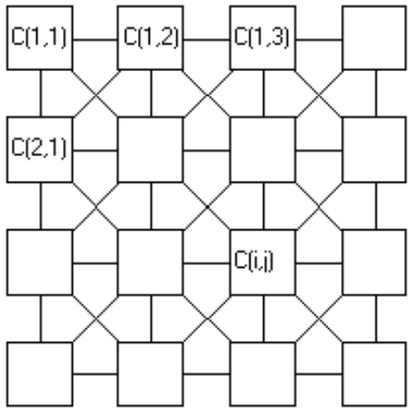

Fig. 3. Architecture of a CNN

If we call the generic cell in the *MxN* array as C_{ij} (the cell on the *i*-th row and the *j*-th column of the array), a formal definition of the neighbourhood of radius *r* of the cell C*ij*, $N_{r(i,j)}$, is given by:

$$N_r(i,j) = \left\{ C_{kl} : max\left\{ \left(k - i\right), \left(l - j\right) \right\} \le r, 1 \le k \le M, 1 \le l \le N \right\} \tag{1}$$

An *MxN* CNN, with *MxN* cells arranged in *M* rows and *N* columns, is entirely characterized by a set of *MxN* non-linear differential equations, associated with each cell. The generic cell x_{ij} is described by the following relations:

$$\begin{aligned} C\frac{dv_{x_{ij}}(t)}{dt} &= -R^{-1}v_{x_{ij}}(t) + \sum_{kl\in N_r} A_{ij,kl}v_{y_{kl}}(t) + \sum_{kl\in N_r} B_{ij,kl}v_{u_{kl}}(t) + I_{ij} \\ &+ \sum_{kl\in N_r} AI_{ij,kl}\left(\Delta v_{yy}\right) + \sum_{kl\in N_r} BI_{ij,kl}\left(\Delta v_{uu}\right) + \sum_{kl\in N_r} D_{ij,kl}\left(\Delta v\right) \\ v_{y_{ij}}(t) &= f\left(v_{y_{ij}}(t)\right) = 0.5\left(\left(v_{x_{ij}}(t)+1\right) - \left(v_{x_{ij}}(t)-1\right)\right) \end{aligned} \tag{2}$$

where:

$$\Delta v_{yy} = v_{y_{kl}}(t) - v_{y_{ij}}(t)$$
$$\Delta v_{uu} = v_{u_{kl}} - v_{u_{ij}}$$
$$\Delta v = v_{u,x,y_{kl}}(t) - v_{u,x,y_{ij}}(t) \quad (3)$$
$$\left(v_{x_{ij}}(t)\right(\le 1, \left(v_{u_{ij}}\right(\le 1, \left(I_{ij}\right(\le v_{max}$$
$$1 \le i \le M, 1 \le j \le N$$

where $v_{x_{ij}}$, $v_{u_{ij}}$, $v_{y_{ij}}$ are respectively the state, input and output voltage of the CNN cell.

The state and output vary in time, whereas the input is kept constant. The indexes *ij* refer to the position of the cell in the 2D grid, while $kl \in N_r$ is a grid point in the neighborhood within the radius *r* of the cell *ij*. Matrices ***A***, ***B***, ***A1***, ***B1***, ***D***, called *templates*, describe the interaction of the cell with its neighbourhood and regulate the evolution of the CNN state and output vectors. Template connections can be realised by voltage-driven current generators.

$A_{ij,kl}$ is called linear feedback template, $B_{ij,kl}$ the linear control template, I_{ij} is a current bias in the cell. $A1_{ij,kl}$, $B1_{ij,kl}$ and $D_{ij,kl}$ are non-linear templates respectively applied to Δv_{yy} , Δv_{uu} and Δv . $A1_{ij,kl}$ is called difference controlled nonlinear feedback template, $B1_{ij,kl}$ is the difference controlled non-linear control template, $D_{ij,kl}$ is the generalized non-linear generator. The output characteristic *f* adopted is a sigmoid-type piecewise-linear function.

CNNs are exploited for image processing by associating each pixel of the image to the input or initial state of a single cell. Subsequently, both the state and output of the CNN matrix evolve to reach an equilibrium state. The evolution of the CNN is governed by the choice of the template. A lot of templates have already been defined in order to perform basic image processing operations, like gradient computation, smoothing, hole detection, line deletion, isolated pixel extraction and deletion, and so on. Simple operations can be performed just by using the basic templates ***A***, ***B***, and the bias ***I***, whereas more complicated processing requires the use of the nonlinear templates ***A1***, ***B1***, and the generalized nonlinear generator ***D***. The proposed algorithm can be totally implemented onto a "*CNN Universal Machine*" (CNN-UM), an hardware structure able to implement CNNs (Chua & Roska, 1993).

The main advantage of using CNNs in image processing is related to the increasing of throughput due to the massive parallelism of the structure, joined to the similar way of signal processing, typical of CNNs. In fact they are able to perform a complete image processing analysis in time of order of 10^{-6} s (by using a CNN hardware implementation), this in form of sequences of simple tasks like array target segmentation, background intensity extraction, target detection and target intensity extraction.

Depending on the type of neurons that are basic elements of the network, it is possible to distinguish continuous-time CNN (CTCNN), discrete-time CNN (DTCNN) (oriented especially on binary image processing), CNN based on multi-valued neurons (CNN-MVN) and CNN based on universal binary neurons (CNN-UBN). CNN-MVN makes possible processing, which is defined by some multiple-valued threshold functions, and CNN-UBN allows processing defined not only by threshold, but also by arbitrary boolean function.

4. The fingerprint verification system

Scale Invariant Feature Transform (SIFT) (Lowe, 2004) was originally developed for general purpose object recognition. SIFT detects stable feature points in an image and performs matching based on the descriptor representing each feature point.

Even though SIFT was originally developed for general purpose object recognition and does not require image preprocessing, we have performed a few preprocessing steps on fingerprint images to obtain better matching performance. The preprocessing is performed in two steps: i) adjusting the graylevel distribution (Csapodi & Roska, 1996) ii) defining a bounding box search area to filter the boundary points of fingerprint. When the fingerprint images show similar texture, the performance is expected to be improved because SIFT uses texture information both for extracting feature points and matching. First, to overcome some apparent differences in gray level distributions, we consider the "image intensity" and adjust the histogram. Second, the boundary area of a fingerprint always causes some feature points to be detected because they are local extrema.

However, the boundary region is different for every fingerprint impression even for the same finger. Therefore, feature points on the fingerprint boundary usually result in false matches. We construct a binary mask that includes only the inner part of a fingerprint and use it to prevent any noisy feature points from being detected on the boundary. In fig.4 is shown a schematic representation of the our algorithm.

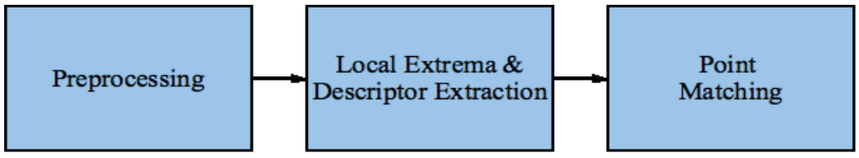

Fig. 4. Flow chart of fingerprint matching using SIFT operator

The feature points are detected using a cascade filtering approach to identify candidate locations that are then examined in further detail. The first stage of keypoint detection is to identify locations and scales that can be assigned under differing "views" of the same object. Detecting locations that are invariant to scale change of the image can be accomplished by searching for stable features using a continuous function of scale known as scale space (Witkin, 1983).

To obtain a scale space (see fig. 2) the initial image is incrementally convolved with Gaussians to produce images separated by a constant factor $\boldsymbol{k}$ in scale space, shown stacked in the left column of fig. 2. Adjacent image scales are subtracted to produce the difference-of-Gaussian images ($\boldsymbol{DOG}$) shown on the right of fig. 2. The set of Gaussian-smoothed images and DOG images are called an octave. Once a complete octave has been processed, we resample the Gaussian image that has twice the initial value of $\boldsymbol{\sigma}$ by taking every second pixel in each row and column. As stated in (Park, 2008) a typical number of scales and octaves for SIFT operation is 5 and 6, respectively.

In a CNN, an implementation of the Gaussian filter with aperture $\boldsymbol{\sigma}$ can be obtained using the *Heat Diffusion* template (Rekeczky et al., 1998; 1999) with *ad hoc* diffusion coefficient (Roska, 1999). As pointed out by Witkin (Witkin, 1983), convolution of the original signal with Gaussians at each scale is equivalent to solving the heat equation with the original image as initial condition.

An example of Heat Diffusion template is as follow:

$$\mathbf{A} = \begin{bmatrix} 0.1 & 0.15 & 0.1 \\ 0.15 & 0 & 0.15 \\ 0.1 & 0.15 & 0.1 \end{bmatrix} \quad \mathbf{B} = \begin{bmatrix} 0 & 0 & 0 \\ 0 & 0 & 0 \\ 0 & 0 & 0 \end{bmatrix} \quad z = \boxed{0} \tag{4}$$

where z is the central element of the matrix $\boldsymbol{I}$ (see eq. 2).
In fig. 5 is shown the obtained results applying the Heat Diffusion template on an image of example.

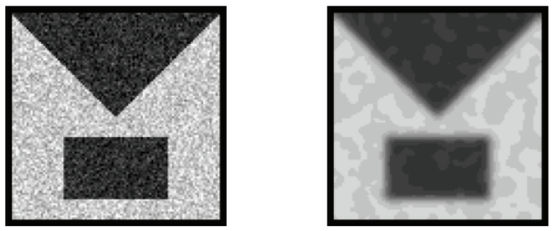

Fig. 5. An example of use of the *Heat Diffusion* template

The standard deviation of the Gaussian filter depend on the a_{ij} matrix elements.
Also, to obtain a difference image it's possible to use the technology described in (Sadeghi-Emamchaie, 1998), where a locally connected analog cellular neural networks (CNNs) is used to implement digital arithmetic arrays; the arithmetic is implemented using a Double-Base Number System (DBNS). Specifically, a CNN array, using a simple non-linear feedback template, with hysteresis, can perform arbitrary length arithmetic with good performance in terms of stability and robustness.
In according to (Lowe, 2004), to obtain a number of feature points we detect the local maxima and minima of the DOG images; each sample point is compared to its eight neighbours in the current image and nine neighbours in the scale above and below (see fig. 2). A feature point is selected only if it is larger than all of these neighbours or smaller than all of them. Then, the same technique is applied for the higher (and lower) octave.
If the first octave is sampled at the same rate as the input image, the highest spatial frequencies will be ignored. This is due to the initial smoothing, which is needed to provide separation of peaks for robust detection.
Therefore, we expand the input image by a factor of 2, using an algorithm of interpolation, prior to building the scale space. In a CNN, an implementation of an algorithm of interpolation (Roska, 1999) can be obtained using the following template:

$$\mathbf{A} = \begin{bmatrix} 0 & 0 & -2 & 0 & 0 \\ 0 & -4 & 16 & -4 & 0 \\ -2 & 16 & -39 & 16 & -2 \\ 0 & -4 & 16 & -4 & 0 \\ 0 & 0 & -2 & 0 & 0 \end{bmatrix} \quad \mathbf{B} = \begin{bmatrix} 0 & 0 & 0 & 0 & 0 \\ 0 & 0 & 0 & 0 & 0 \\ 0 & 0 & 0 & 0 & 0 \\ 0 & 0 & 0 & 0 & 0 \\ 0 & 0 & 0 & 0 & 0 \end{bmatrix} \quad z = \boxed{0} \tag{5}$$

In fig. 6 we show an example of interpolation obtained with this template.
The local maximum (and minimum) in a given neighbourhood (see fig. 7) can be computed using a single layer CNN through a difference-controlled template (***Local maxima detector***

template), as described in (Chua et al., 1993). Each local minimum can also be detected if the input image is inverted. However an improvement of the performances can be obtained using a local maxima detector based on multi-layer CNN (Roska & Chua, 1993).

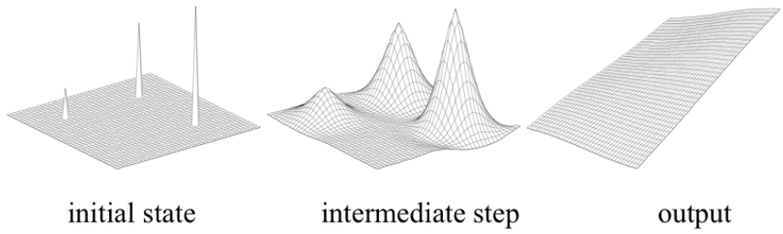

Fig. 6. Fitting a surface on three given points. Image size: 80x80.

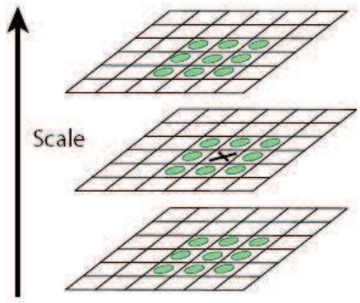

Fig. 7. Maxima and minima of the difference-of-Gaussian images are detected by comparing a pixel (marked with X) to its 26 neighbours in 3x3 regions at the current and adjacent scales (marked with circles).

A local extrema is observed if its derivative in scale space is stable and if it is on an apparent edge. If an extremum is decided as unstable or is placed on an edge, it is removed because it can not be reliably detected again with small deformations or lighting changes.
To remove the extremum placed on an edge we use a mask image obtained processing the input image with an edge-detector described in (Roska, 1999). Then, the next step is to reject the points that have low contrast (and are therefore sensitive to noise).
In order to reject the points that have low contrast we use a mask image obtained processing the input image with the technique introduced in (Cserey et al., 2003). In this approach a parallel histogram modification technique based on embedded morphological pre-processing is formulated in terms of non-linear partial differential equations (PDE).
Now, to characterize the image at each key location (keypoint), the first smoothed image at each octave of the pyramid is processed to extract image gradients and orientations.
In a CNN, the estimation of the gradient intensity in a local neighbourhood can be obtained using the following template:

$$\mathbf{A} = \begin{bmatrix} 0 & 0 & 0 \\ 0 & 0 & 0 \\ 0 & 0 & 0 \end{bmatrix} \quad \mathbf{B} = \begin{bmatrix} b & b & b \\ b & 0 & b \\ b & b & b \end{bmatrix} \quad z = \boxed{0} \tag{6}$$

where $b = |vuij - vukl|/8$.

To each key location is assigned a "canonical orientation", so that the image descriptors are invariant to rotation. This orientation is estimated by the gradient orientations of sample points within a region around the keypoints. To make the descriptor stable against lighting or contrast changes, the orientation is determined as follow:

- we estimate the gradient orientation of the pixels, within a region around the keypoint, applying a grayscale line detector template (8 *templates* for 8 *directions*) presented in (Roska, 1999);
- we add the 8 ***maps*** obtained (***SUM*** – to each pixel of the image we have an estimate of its orientation);
- we obtain an image ***mask*** applying the mathematical morphology operator dilation (Roska, 1999) on an image that contains only keypoints (***keypoints mask***). The mask locates the points that will contribute to the estimate of the ***keypoints orientation***;
- we calculate the local mean (neighbourhood – 3x3) of the image ***SUM*** (Moreira-Tamayos & Gyvez, 1999) on the points "selected" by the mask image.

The orientations estimated correspond to dominant directions of local gradients. Given a stable location, scale, and orientation for each key, it is now possible to describe the local image region in a manner invariant to these transformations. In addition, it is desirable to make this representation robust against change in lighting and small shifts in local geometry, such as arise from affine.

One obvious approach would be to sample the local image intensities around the keypoint at the appropriate scale, and to match these using a normalized correlation measure. However, simple correlation of image patches is highly sensitive to changes that cause misregistration of samples, such as affine or non-rigid deformations.

In according to (Park, 2008), now we generate a map of gradient orientations around each local extremum and then to make the descriptor orientation invariant, all gradient orientations are rotated respect to the major orientation (***keypoints orientation***) of the local extremum.

To obtain a ***local map*** of gradient orientation we proceed as follow:

- we calculate the gradient intensity of the fingerprint image;
- we use the grayscale line detector templates (8 orientation images, applied only on the keypoints neighbourhood – size: 16x16);
- we add the 8 orientation images to obtain a ***local gradient orientation image***;
- we calculate the difference (**SUB**) between the local gradient orientation image and the keypoints orientation image (***canonical orientation of the keypoints***), the **SUB** image contains the gradient orientations rotated respect to the keypoints orientation;
- we calculate a weighted mean (Moreira-Tamayos & Gyvez, 1999) of the **intensity gradient image** and of the "rotated" **local gradient orientation image**.

In the original implementation (Lowe, 1999) of SIFT the best candidate match for each keypoint is found by identifying its nearest neighbour in the database of keypoints from training images. The nearest neighbour is defined as the keypoint with minimum Euclidean distance for the invariant descriptor vector. To obtain more details on matching process read (Lowe, 2004).

In our tests we used two metrics:

- the original solution described in (Lowe, 1999);
- the metric described in (Szatmári, 2006).

The first solution is more accurate (see Section 5) but it's not implemented on a CNN. The second metric though implemented on CNN, indeed, is less accurate, reliable and robust.

In (Szatmári, 2006) the author investigated PDE-based dynamic phenomena for comparing objects and introduced a spatio-temporal non-linear wave metric. This metric is capable of comparing both binary and gray-scale object pairs in a parallel way. Spatio-temporal waves are controlled to explore the quantitative properties of objects. In addition to spatial data time related information is also extracted and used for evaluating differences and similarities. The detailed analysis of the proposed metric shows that this wave-based approach can outperform well-known metrics such as Hausdorff and Hamming metrics in selectivity and sensitivity.

5. Experimental results

In according to (Park, 2008), the performances of the proposed SIFT based fingerprint verification has been evaluated on FVC2002 DB1 and DB2 fingerprint databases (Maio, 2002). Both the databases contain images of 100 different fingers with 8 impressions for each finger. In FVC2002 project, a total of ninety students (20 years old on the average) enrolled in the first two years of a Computer Science degree program agreed to act as volunteers for providing fingerprints. The volunteers were randomly partitioned into different groups, each group was associated to a DB and therefore to a different fingerprint scanner. Forefinger and middle finger of both the hands (four fingers total) of each volunteer were acquired by interleaving the acquisition of the different fingers to increase differences in finger placement. The top-ten quality fingers were removed from each database since they do not constitute an interesting case study. The remaining 110 fingers were split into set A (100 fingers - evaluation set) and set B (10 fingers - training set). To make set B representative of the whole database, the 110 collected fingers were ordered by quality. During a session, fingers were alternatively dried and moistened.
Some characteristics of these two databases are summarized in table 1.

	Sensor Type	Image Size	Images	Resolution
DB1	Optical Sensor	388x374	100x8	500 dpi
DB2	Optical Sensor	296x560	100x8	569 dpi

Table 1. Description of FVC 2002 DB1 and DB2 databases

The performance of the whole system, was evaluated by the Equal Error Rate (EER) for each metric used (see table 2). At Equal Error Rate, FAR=FRR. As the name implies, the FAR (False Acceptance Rate) describes the ability of the system to reject fingerprints which are not allowed to access the system, while the FRR (False Rejection Rate) describes the ability of the system to accept fingerprints which belong to the system users.

	EER1	EER2
DB1	9.30%	9.67%
DB2	11.65%	12.36%

Table 2. Description of the experimental results. EER1 and EER2 are, respectively, the equal error rate with the Lowe's metric and the Szatmári's metric.

As stated in section 4, the first metric is more accurate but it's not implemented on CNNs (*therefore with a lower matching speed*).

6. Conclusion

In this chapter we re-formulate an algorithm for fingerprint verification using the Scale Invariant Feature Transform (SIFT) (Lowe, 2004; Park et al., 2008) in such a way to exploit the high degree of parallelism inherent in a single-layer CNN. In our implementation we extract characteristic SIFT feature points in scale space and perform a matching based on the texture information around the feature points using the SIFT operator (Chikkerur, 2006). Experimental measures of the accuracy of the our fingerprint verification system were carried out.

7. References

Bálya, D. (2003). CNN universal machine as classification platform: an art-like clustering algorithm. *Int. J. Neural Syst.*, Vol. 13, No. 6, December 2003, pp. 415-425.

Bicego, M.; Lagorio, A.; Grosso, E. & Tistarelli, M. (2006). On the Use of SIFT Features for Face Authentication, *Proceedings of CVPRW'06*, pp. 35, 0-7695-2646-2, IEEE Computer Society, New York, NY.

Chikkerur, S.; Pankanti, S.; Jea, A.; Ratha, N. & Bolle, R. (2006). Fingerprint Representation Using Localized Texture Features. *Proceedings of ICPR 2006*, pp. 521-524, 1051-4651, August 2006, IEEE Computer Society, Hong Kong, China.

Chua, L. & Yang, L. (1988). Cellular neural networks: Theory, *IEEE Trans. on Circuits and Systems*, Vol. 35, No. 10, pp. 1257–1272.

Chua, L. & Yang, L. (1988). Cellular neural networks: Applications, *IEEE Trans. on Circuits and Systems*, Vol. 35, No. 10, pp. 1273–1290.

Chua, L.O.; Roska, T.; Kozek, T. & Zarándy, Á. (1993). The CNN Paradigm − A Short Tutorial, *Int. J. Circuit Theory and Applications*, Cellular Neural Networks Special Issue, 1993, pp. 1-14, 0-471-93836-X.

Costantini, G.; Casali, D.; Carota, M. & Perfetti, R. (2004). Translation and Rotation of Grey-Scale Images by means of Analogic Cellular Neural Network. *Proceedings of the IEEE International Workshop on Cellular Neural Networks and their Applications (CNNA'2004)*, pp. 213-218, 963-311-357-1, IEEE Computer Society, Budapest, Hungary.

Csapodi, M. & Roska, T. (1996). Adaptive histogram equalization with Cellular Neural Networks. *Proceedings of CNNA'96*, pp. 81-86, 0-7803-3261-X, , Seville, Spain.

Cserey, G.; Rekeczky, C. & Földesy, P. (2003). PDE Based Histogram Modification With Embedded Morphological Processing of the Level-Sets, *Journal of Circuits, System and Computers*, Vol. 12, No. 4, August 2003, pp. 519-538.

Gao, Q.; Förster, P.; Möbus, K.R. & Moschytz, G.S. (2001). Fingerprint Recognition Using CNNs: Fingerprint Preprocessing, *Proceedings of IEEE International Symposium on Circuits and Systems*, pp. 433-436, 0-7803-6685-9, May 2001, IEEE Computer Society, Sydney, Australia.

Gao, Q. & Moschytz, G.S. (2001). Fingerprint Feature Extraction Using CNNs, *Proceedings of European Conference on Circuit Theory and Design*, pp. 97-100, 9-5122-6337-8, August 2001, Espoo, Finland.

Gao, Q. &. Moschytz, G.S (2004). Fingerprint Feature Matching Using CNNs, *Proceedings of ISCAS'04*, pp. 73-76, 0-7803-8251-X, May 2004, IEEE Computer Society, Vancouver, Canada.

Huttenlocher, D.; Klanderman, G. & Rucklidge, A. (1993). Comparing images using the hausdorff distance, *IEEE Transactions on Pattern Analysis and Machine Intelligence*, Vol. 15, No. 9, (September 1993),pp. 850–863.

Iannizzotto, G.; Lanzafame, P. & La Rosa, F. (2005). A CNN-based Framework for 2D Still-image Segmentation, *Proceedings of CAMP05*, pp. 210-215, 0769522556, Terrasini, July 2005, IEEE Computer Society, Palermo, Italy.

Jain, A.K.; Hong, L. & Bolle, R. (1997). On-line fingerprint verification, *IEEE Transactions on Pattern Analysis and Machine Intelligence*, Vol. 19, April 1997, pp. 302-314, 0162-8828.

Lowe, D. (2004). Distinctive image features from scale-invariant key points. *International Journal of Computer Vision*, Vol. 60, No. 2, pp. 91-110.

Lowe, D. (1999). Object Recognition from Local Scale-Invariant Features. *Proceedings of ICCV'99*, pp. 1150-1157, 0-7695-0164-8, IEEE Computer Society, Kerkyra, Greece.

Maio, D.; Maltoni, D.; R. Cappelli; Wayman, J.L. & Jain, A.K. (2002). FVC2002: Second Fingerprint Verification Competition. *Proceedings of ICPR'02*, pp., 0-7695-1695-X, IEEE Computer Society, Quebec City, Canada.

Milanova, M. & Buker, U. (2000). Object recognition in image sequences with cellular neural networks, *Neurocomputing*, Vol. 31, No. 1-4, March 2000, pp. 125–141.

Moreira-Tamayos, O. & Gyvez, J. P. D. (1999). Subband coding and image compression using cnn, *International Journal of Circuit Theory and Applications*, Vol. 27, No. 1, March 1999, pp. 135–151, 0098-9886.

Park, U.; Pankanti, S. & Jain, A.K. (2008). Fingerprint Verification Using SIFT Features. *Proceedings of SPIE Defense and Security Symposium*, 0277-786X, SPIE, Orlando, Florida.

Ratha, N. K.; Karu, K. ; Chen, S. & Jain, A. K. (1996). A Real-Time Matching System for Large Fingerprint Databases, *IEEE Transactions on Pattern Analysis and Machine Intelligence*, Vol. 18, No. 8, August 1996, pp. 799–813, 0162-8828.

Rekeczky, C.; Tahy, A.; Vegh, Z. & Roska, T. (1999). CNN based spatio-temporal nonlinear filtering and endocardial boundary detection in echocardiography. *International Journal of Circuit Theory and Applications*, Vol. 27, No. 1, March 1999, pp. 171 – 207, 0098-9886.

Roska, T. & Chua, L.O. (1993). The CNN universal machine: an analogic array computer. IEEE Transactions on Circuits and Systems II: Analog and Digital Signal Processing, Vol. 40, No. 3, March 1993, pp. 163 – 173.

Roska, T.; Kek, L. ; Nemes, L.; Zarandy, A. & Szolgay, P. (1999). CNN Software Library (templates and algorithms), vers. 7.3. Tech. Rep. DNS-CADET-15. Analogical & Neural Computing Laboratory. Computer and Automation Research Institute, Hungarian Academy of Sciences.

Rekeczky, C.; Roska, T. & Ushida A. (1998). CNN-based difference-controlled adaptive nonlinear image filters. *International Journal of Circuit Theory and Applications*, Vol. 26, July-August 1998, pp. 375-423.

Sadeghi-Emamchaie, S.; Jullien, G.A.; Dimitrov, V. & Miller, W.C. (1998). Digital Arithmetic Using Analog Arrays. *Proceedins of the Great Lakes Symposium on VLSI '98*, p. 202, 0-8186-8409-7, IEEE Computer Society, Lafayette, LA, USA.

Szatmári, I. (2006). Object comparison using PDE-based wave metric on cellular neural networks. *International Journal of Circuit Theory and Applications, Vol. 34, No. 4, June 2006, pp. 359 – 382.*

Su, T.; Du, Y.; Cheng, Y. & Su, Y. (2005). A Fingerprint Recognition System Using Cellular Neural Networks. *Proceedings of Int'l Workshop on Cellular Neural Networks and Their Applications*, pp. 170-173, 0-7803-9185-3, IEEE Computer Society, Istanbul, Turkey.

Szirànyi, T. & Csicsvàri, J. (1993). High-speed character recognition using a dual cellular neural network architecture (cnnd), *IEEE Transactions on Circuits and Systems II: Analog and Digital Signal Processing*, Vol. 40, No. 3, March 1993, pp. 223–231, 1057-7130.

Theodoridis, S. & Koutroumbas, K. (2006). Pattern Recognition. Academic Press, 0-12-369531-7.

Witkin, A.P. (1983). Scale-space filtering. *Proceedings of International Joint Conference on Artificial Intelligence*, pp. 1019-1022, Karlsruhe, Germany.

Pattern Recognition Techniques, Technology and Applications

Edited by Peng-Yeng Yin

ISBN 978-953-7619-24-4
Hard cover, 626 pages
Publisher InTech
Published online 01, November, 2008
Published in print edition November, 2008

A wealth of advanced pattern recognition algorithms are emerging from the interdiscipline between technologies of effective visual features and the human-brain cognition process. Effective visual features are made possible through the rapid developments in appropriate sensor equipments, novel filter designs, and viable information processing architectures. While the understanding of human-brain cognition process broadens the way in which the computer can perform pattern recognition tasks. The present book is intended to collect representative researches around the globe focusing on low-level vision, filter design, features and image descriptors, data mining and analysis, and biologically inspired algorithms. The 27 chapters coved in this book disclose recent advances and new ideas in promoting the techniques, technology and applications of pattern recognition.

INTECH
open science | open minds

InTech Europe
University Campus STeP Ri
Slavka Krautzeka 83/A
51000 Rijeka, Croatia
Phone: +385 (51) 770 447
Fax: +385 (51) 686 166
www.intechopen.com

InTech China
Unit 405, Office Block, Hotel Equatorial Shanghai
No.65, Yan An Road (West), Shanghai, 200040, China
中国上海市延安西路65号上海国际贵都大饭店办公楼405单元
Phone: +86-21-62489820
Fax: +86-21-62489821

IntechOpen